Journal of
Materials Chemistry B

Materials for biology and medicine

Accepted Manuscript

This article can be cited before page numbers have been issued, to do this please use: F. Wang, Y. Wang, J. Xu and K. Huang, *J. Mater. Chem. B*, 2020, DOI: 10.1039/C9TB02574J.

ROYAL SOCIETY OF CHEMISTRY

rsc.li/materials-b

View Article Online
DOI: 10.1039/C9TB02574J

High-energy sandwiched-type self-powered biosensor based on DNA bioconjugates and nitrogen doped ultra-thin carbon shell

Fu-Ting Wang, Yi-Han Wang, Jing Xu, Ke-Jing Huang*

College of Chemistry and Chemical Engineering, Xinyang Normal University, Xinyang 464000, China

*Corresponding author.

E-mail address: kejinghuang@163.com (K.J. Huang)

View Article Online
DOI: 10.1039/C9TB02574J

Abstract

A high-energy self-powered sensing platform for ultrasensitive detection of protein is developed based on enzymatic biofuel cells (EBFCs) by using DNA bioconjugates assisted signal amplification. Nitrogen doped ultra-thin carbon shell/gold nanoparticles (N-UHCS/AuNPs) composite is prepared and applied as electrode supporting substrate to improve enzyme load. The biocathode of self-powered sensor is constructed through step by step modifying N-UHCS/AuNPs and bilirubin oxidase (BOD) on the carbon paper (CP). For fabricating the bioanode, SiO_2 nanospheres@AuNPs-aptamer (SiO_2@AuNPs-ssDNA) bioconjugates are prepared and modified on CP. When the target protein exists, the aptamer recognizes it and therefore makes SiO_2@AuNPs-ssDNA bioconjugate fall off from the bioanode, resulting in a significant increase of open circuit voltage (E^{OCV}) of the sensing device. Under optimal conditions, the developed biosensor shows a wide linear range of 0.1-2000 ng mL^{-1} with a low detection limit of 21.5 pg mL^{-1} (S/N=3). This work shows an effective assay for sensitively detection of biomolecules by coupling the EBFCs, DNA bioconjugates and biosensing characteristics of smart nanostrutures.

Keywords: Self-powered biosensor; Enzyme biofuel cells; DNA bioconjugates; Protein; Sensitive detection; Signal amplification

View Article Online
DOI: 10.1039/C9TB02574J

1. Introduction

Enzymatic biofuel cell (EBFC) is drawing wide concern because of its moderate operation conditions and promising applications as implantable power devices.[1,2] Currently, the development of EBFCs mainly focuses on preparation of new device that has big power output and good stability, and devotes to developing the new applications, such as self-powered sensors,[3-6] immunoassays system[7,8] and cytosensing devices.[6,9,10] Among them, the EBFC based self-powered sensors usually possess unique advantages of no needing external power supplys, low cost, relatively small size and simple fabrication process.[4,11-13] However, the biorecognition of the EBFC based self-powered biosensors by enzymes or oligonucleotide probe usually requires complicated experimental steps,[14, 15] leading to the poor stability and low enzyme loading capacity and therefore obviously damages their performance. Thus, it is very important to fabricate new sensing platforms integration of EBFC and nanomaterials with high specific surface area and good conductivity for expanding the enzyme loading quantities and improving analytical performance.

Carbon materials with big surface areas and good electrical conductivity have been widely used in electrochemical biosensors.[16,17] Usually doping carbon materials with heteroatoms can not only prevent the restacking of the sheets but also further improve the electrical conductivity, specific surface area, the charge density of state and wettability of the electrode.[18-20] Au nanoparticles (AuNPs) have been widely used in the fabrication of biosensor due to their excellent conductivity and the ability of immobilizing biomolecular by Au-S bond.[21] DNA is an important genetic molecule

View Article Online
DOI: 10.1039/C9TB02574J

and has been widely used in the fabrication of biosensor.[21-23] Since DNA is a densely charged polyelectrolyte, self-assembly of DNA sequences on nanostructure usually shows good stability than pure DNA molecule due to strong inter-particle electrostatic repulsion.

Platelet-derived growth factor BB (PDGF-BB) has been reported as an important tumor marker.[24,25] In this work, an ultrasensitive EBFCs based self-powered aptasensor is fabricated for PDGF-BB analysis. Ultra-thin nitrogen doped carbon shell/gold nanoparticles (N-UHCS/AuNPs) is prepared as electrode supporting substrate. The biocathode of the EBFCs is constructed through step by step modifying N-UHCS/AuNPs and bilirub in oxidase (BOD) on the carbon paper (CP). For fabricating the bioanode, the SiO_2@gold nanoparticles-aptamer (SiO_2@AuNPs-ssDNA) was elaborately designed and prepared by anchoring ssDNA to the surface of SiO_2@AuNPs via Au-S bond. In the absence of PDGF-BB, a low open circuit voltage (E^{OCV}) is obtained due to the effect of steric hindrance. When PDGF-BB is added, SiO_2@AuNPs-ssDNA falls away from the bioanode because of the recognizing PDGF-BB by DNA1. Thus glucose can reach the active sites of GOD and a greatly improved E^{OCV} is achieved. This bioassay needs no external power supply and shows high sensitivity and selectivity, exhibiting a great promise as a powerful tool for sensitive detection of tumor markers.

2. Experimental

2.1. Chemicals and reagents

View Article Online
DOI: 10.1039/C9TB02574J

Bilirubin oxidase (BOD), Glucose-oxidase (GOD), poly (diallyldimethylammonium chloride) (PDDA), 3-aminopropyltrimethoxysilane (APTMS), chlorauric acid ($HAuCl_4 \cdot 3H_2O$), and 6-mercaptol-1-hexyl alcohol (MCH) were obtained from Aladdin Co. Ltd. Thrombin (TB) and carcinoembryonic antigen (CEA) were obtained from Beijing Solaibao Technology Co. Ltd. PDGF-BB, aptamer, immunoglobulin G (IgG), ssDNA (5'-SH_2-$(CH_2)_6$-CAGGATCATGGTGATGCTCTACGTGCCGTAGCCTG-3') and DNA1 (5'-SH_2-$(CH_2)_6$-CAGGCTACGGCACGTAGAGCATCACCATGATCCTG-3') were obtained from Shanghai Sangon Bioengineering Co. Ltd.

2.2. Instrumentation

Electrochemical detection was performed on a CHI660E electrochemical workstation (Shanghai CH Instruments Co. Ltd. China). The EIS detection was carried out in 0.1 M PBS (pH=7.4)) with 5.0×10^{-3} mol L^{-1} potassium ferricyanide and 1.0×10^{-4} mol L^{-1} potassium chloride. The CV was tested in 0.1 M PBS (pH=7.4) with a scan rate of 0.1 V S^{-1}. The working electrode is the fabricated bioanode or biocathode. An Ag/AgCl and a platinum electrode were applied as the reference electrode and the auxiliary electrode, respectively. Scanning electron microscopy (SEM) and transmission electron microscopy (TEM) images were measured on a S-4800 SEM (Hitachi, Japan) and a Tecnai G2 F20TEM (FEI, USA).

2.3. Preparation of N-UHCS/AuNPs

View Article Online
DOI: 10.1039/C9TB02574J

The UHCS was prepared according to the references.[26,27] In short, 3 g sodium citrate was kept under 155 °C in oven for one day and ball-milled for 12 h. Subsequently, the mixture was annealed under N_2 atmosphere at 600 °C for 60 min with a heating rate of 5 °C min^{-1}. Then, the sample was washed with HCl solution and water to neutral. The obtained material was then dried for 24 h at 60 °C to get UHCS. Then, 100 mg UHCS sample was added into a watch glass, then 3 mL triethylamine was injected into the sample and ignition mixture. The black product N-UHCS was collected after the combustion stopped.

The AuNPs were synthesized by reducing $HAuCl_4$ with citrate according to the reference.[28] In brief, 50 mL $HAuCl_4$ (1.0×10^{-3} mol L^{-1}) was heated to boil. 5 mL sodium citrate (4.0×10^{-2} mol L^{-1}) was then rapidly added in. The colour of solution changed to burgundy. The mixture was kept in a boiling state for 10 minutes, and then stirred for 15 minutes. The product was stored at 4°C.

5 mg of N-UHCS was dispersed in 1% PDDA (3 mL) to get positively charged N-UHCS. Residual PDDA was removed by washing with ultrapure water. The functional N-UHCS was mixed with 6 mL AuNPs (with 1 mg mL^{-1} EDC/NHS) and the mixture was gently shaken overnight. After washed with water, the precipitate was resuspended into PBS buffer to obtain the N-UHCS/AuNPs.

2.4. Fabrication of SiO_2@AuNPs-ssDNA

SiO_2 nanospheres were first prepared as follows: 77.5 mL ethanol, 112.5 mL $NH_3\cdot H_2O$, 5 mL tetraethyl orthosilicate and 31.25 mL water were mixed, and stirred

View Article Online
DOI: 10.1039/C9TB02574J

for 180 min to get SiO_2 nanospheres. Excessive $NH_3 \cdot H_2O$ and tetraethyl orthosilicate were removed by centrifugation (6000 rpm, 20 min), and then dried at 60 °C. SiO_2 nanospheres was dispersed in ethanol (20 mL) and then 0.5 mL APTES was dropwise added and stirred for 2 h. The excess APTMS was then removed by centrifugation. Subsequently, 1 mL AuNPs and 500 μL of 1 mg mL^{-1} EDC/NHS were incubated with SiO_2 nanospheres for 24 h to obtain SiO_2@AuNPs. After that, 500 mL of 1 μM ssDNA was added and kept overnight at 4°C. 30 μL of 1 mM MCH was then added and retained for 0.5 h. After washed with PBS, the SiO_2@AuNPs-ssDNA bioconjugate was obtained.

2.5. Preparation of self-powered aptasensor

50 μL of 1 mg mL^{-1} N-UHCS/AuNPs was coated upon carbon paper (CP) electrode (1 cm × 1 cm) and then vacuum dried at 37 °C for 2 h. Subsequently, the electrode was incubated into 1 mg mL^{-1} EDC/NHS for 0.5 h. After rinsed with water, the electrode was immersed in 1 μM aptamer (DNA1) solution (with 30 mg mL^{-1} GOD) and kept overnight at 4 °C to obtain DNA1/GOD/N-UHCS/AuNPs electrode. Subsequently, 50 μL SiO_2@AuNPs-ssDNA bioconjugate was dropped onto the electrode and kept under 37 °C for 1.5 h. The biocathode was prepared by incubating N-UHCS/AuNPs modified CP electrode in 50 μL of 8 mg mL^{-1} BOD overnight at 4 °C. The fabricated aptasensor was incubated with PDGF-BB under 37 °C for 30 min and then the E^{OCV} was measured.

View Article Online
DOI: 10.1039/C9TB02574J

3. Results and discussion

3.1. Design of self-powered aptasensor

The mechanism of the preparation of EBFCs based self-powered aptasensor is shown in Scheme 1. The aptasensor composes of SiO_2@AuNPs–ssDNA/DNA1/GOD/N-UHCS/AuNPs/CP bioanode and BOD/N-UHCS/AuNPs/CP biocathode. When there is no PDGF-BB, SiO_2@AuNPs-ssDNA bioconjugate prevents the electron transfer of the glucose because of steric hindrance effect. A low open circuit voltage (E^{OCV}) is observed. However, when PDGF-BB is added, the aptamer DNA1 captures it and the DNA bioconjugate falls off from the bioanode due to the hybridization of DNA1 and ssDNA. The glucose reaches the active sites of GOD and results in the electron transfer between the glucose and GOD. Thus, a significantly increased E^{OCV} is obtained and sensitive determination of PDGF-BB is realized.

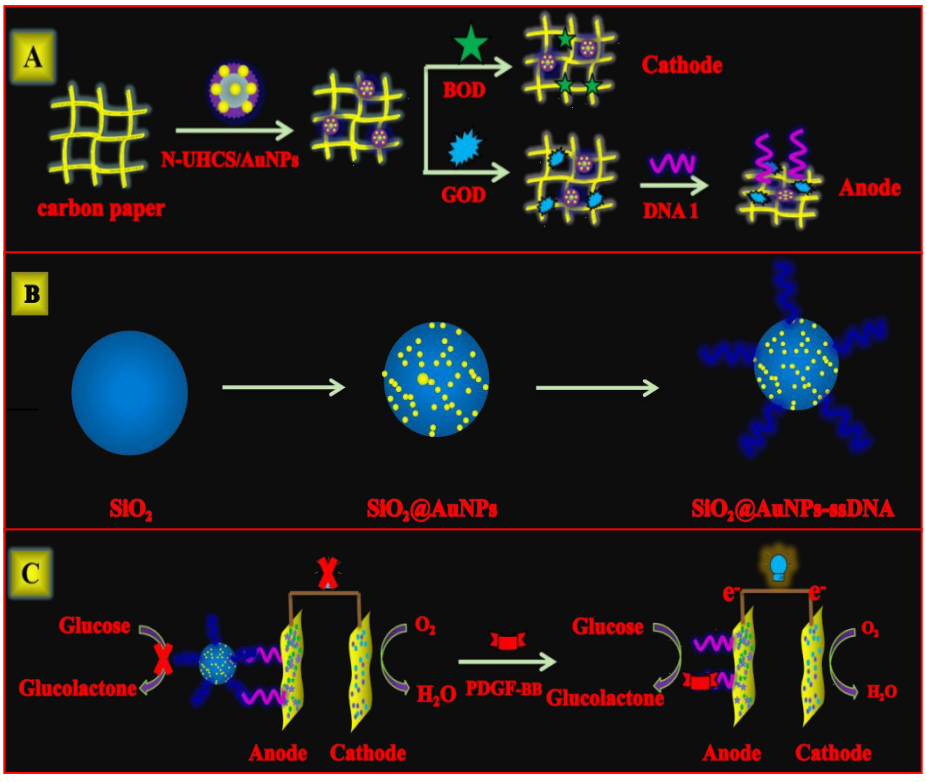

View Article Online
DOI: 10.1039/C9TB02574J

Scheme 1. Schematic illustration of the principle of the self-powered strategy for PDGF-BB detection.

3.2. Characterization of prepared materials

Fig. 1A is a SEM image of N-UHCS, which is observed to be composed of a number of interconnected ultra-thin hollow carbon shells. The white arrows pointing towards their rich hollow structures, which can improve the conductivity of electrons due to the shortened ions diffusion path. As shown in Fig. 1B, the TEM image clearly illustrates the ultra-thin hollow morphology of N-UHCS. Fig. 1C and 1D are the SEM and TEM images of the N-UHCS/AuNPs. It shows that the AuNPs are distributed evenly and densely onto the surface of N-UHCS. Fig. 1E is a SEM image of the N-UHCS/AuNPs/CP. Multiple N-UHCS/AuNPs are decorated on the CP electrode, which is beneficial to immobilize more enzyme and aptamer, so as to further improve detection signal. Fig. 1F is the SEM image of SiO_2 nanosphere, which exhibits a well-defined and highly uniform spherical structure with particle size of about 150 nm.

View Article Online
DOI: 10.1039/C9TB02574J

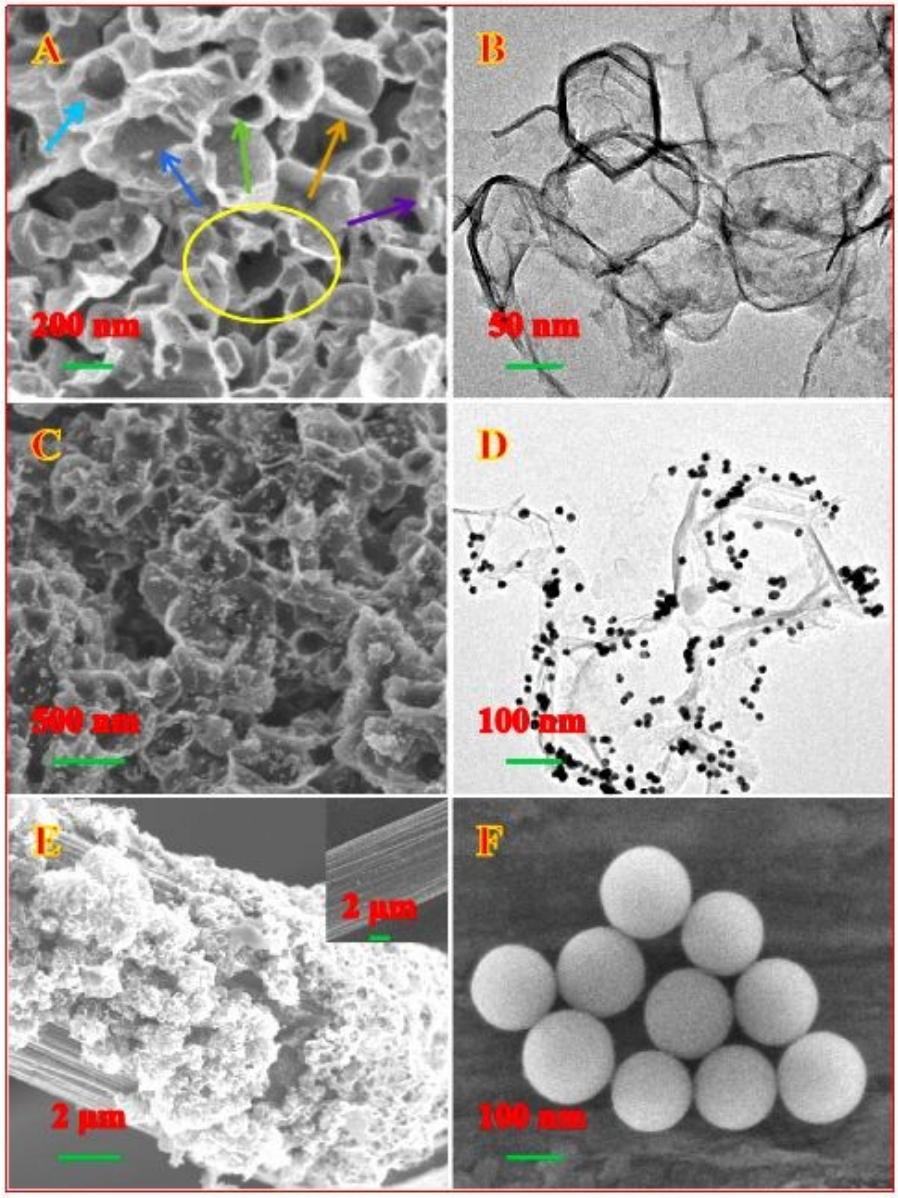

Fig 1. SEM (A) and TEM (B) images of N-UHCS; SEM (C) and TEM (D) images of N-UHCS/AuNPs; SEM image of N-UHCS/AuNPs/CP (E) , the inset is the bare CP; SEM image of SiO_2 (F).

The XRD images of the UHCS, N-UHCS and N-UHCS/AuNPs are shown in Fig. 2A. All samples exhibit a strong diffraction peak at 23°, which comes from (002) planes of graphite.[29] Among them, the XRD pattern of N-UHCS/AuNPs exhibits obvious bands at 38.14°, 44.44°, 64.57° and 77.43°, corresponding to (111), (200),

View Article Online
DOI: 10.1039/C9TB02574J

(220) and (311) crystal planes of Au, respectively.[30] The XPS image of UHCS, N-UHCS and N-UHCS/AuNPs composites are shown in Fig. 2B. C and O elements can be observed in the samples. N element can be obviously found in N-UHCS (Fig. 2B), suggesting the successful doping of the hetero atoms in the sample. N_2 adsorption/desorption isotherms of the UHCS and N-UHCS are shown in Fig. 2C and D. The isotherms are type IV when the relative pressure is between 0.4 and 1.0, indicating UHCS and N-UHCS have a large specific surface and mesoporous feature. The specific surface areas of UHCS and N-UHCS are measured as 182.48 $m^2 g^{-1}$ and 628.89 $m^2 g^{-1}$, and the main pore sizes are 5.78 nm and 6.53 nm, respectively.

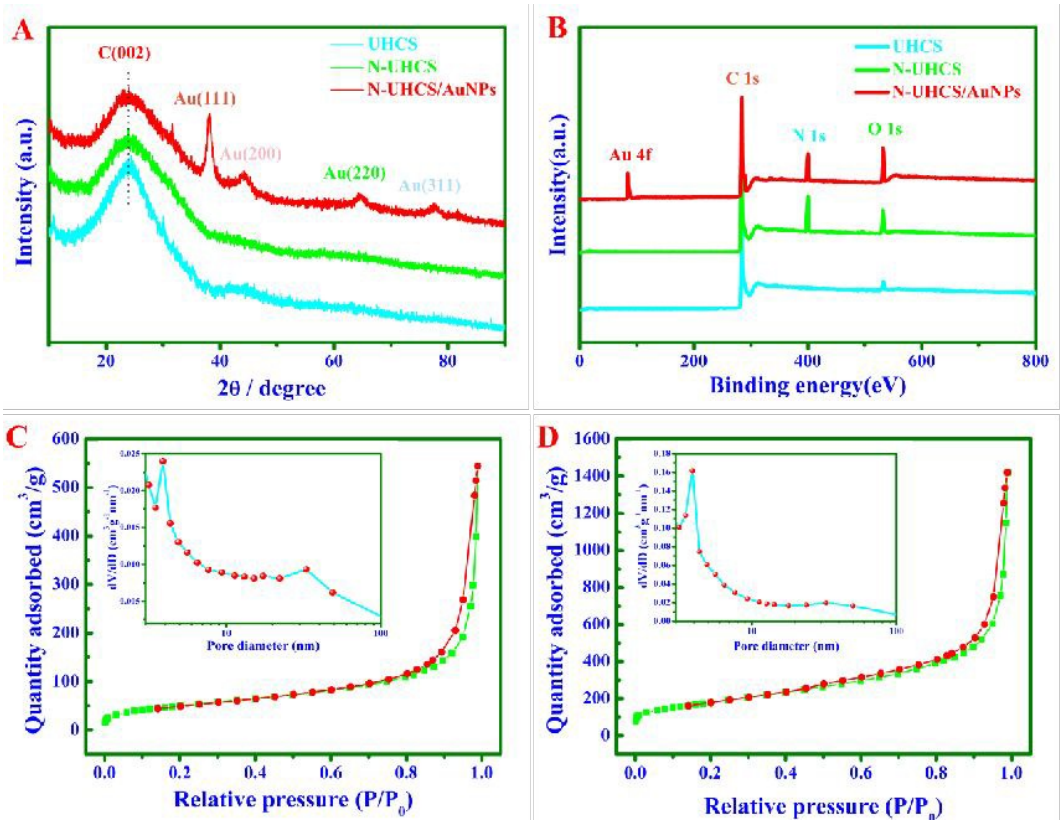

Fig 2. XRD pattern (A) and XPS survey spectra (B) of UHCS, N-UHCS, and N-UHCS/AuNPs; N_2 adsorption/desorption isotherms of UHCS (C) and N-UHCS (D). Inset is the pore size distribution curves.

View Article Online
DOI: 10.1039/C9TB02574J

3.3. Electrochemical behaviour of self-powered biosensor

The assembly process of the bioanode and biocathode was monitored by EIS and CV (Fig. 3). Compared to the bare CP, N-UHCS/AuNPs/CP significantly reduces the semicircle, due to its good conductivity. After BOD is immobilize on the biocathode (curve c), the impedance value increases obviously due to the steric hindrance of the enzyme. After GOD and DNA1 are modified (Fig. 3B, curve c), the semicircle significantly increases due to the abundant negative charge of DNA1 and large steric hindrance of GOD. When the DNA bioconjugate SiO_2@AuNPs-ssDNA is assembled on the bioanode, the semicircle greatly increases (curve d) due to the steric hindrance effects. The appear of target PDGF-BB makes SiO_2@AuNPs-ssDNA bioconjugate falls off from the bioanode, resulting the semicircle significantly reduces (curve e). The EIS results obviously indicates the successful assembly of bioanodes.

As shown in Fig. 3C, compared with that in N_2 electrolyte solution (curve a), cathodic currents greatly improved in the air or O_2 saturated electrolyte solution, indicating BOD/N-UHCS/AuNPs/CP biocathode has highly efficient catalytic activity towards oxygen reduction. In Fig. 3D, there is no redox peak is observed on bioanode when there is no PDGF-BB. In the absence or presence of glucose, the redox peaks of the bioanode appears at about -0.5 V (curve a, b), which is the characteristic peak of GOD. When 0.1 μg mL^{-1} PDGF-BB is added, the current signal significantly increases (curve c).

View Article Online
DOI: 10.1039/C9TB02574J

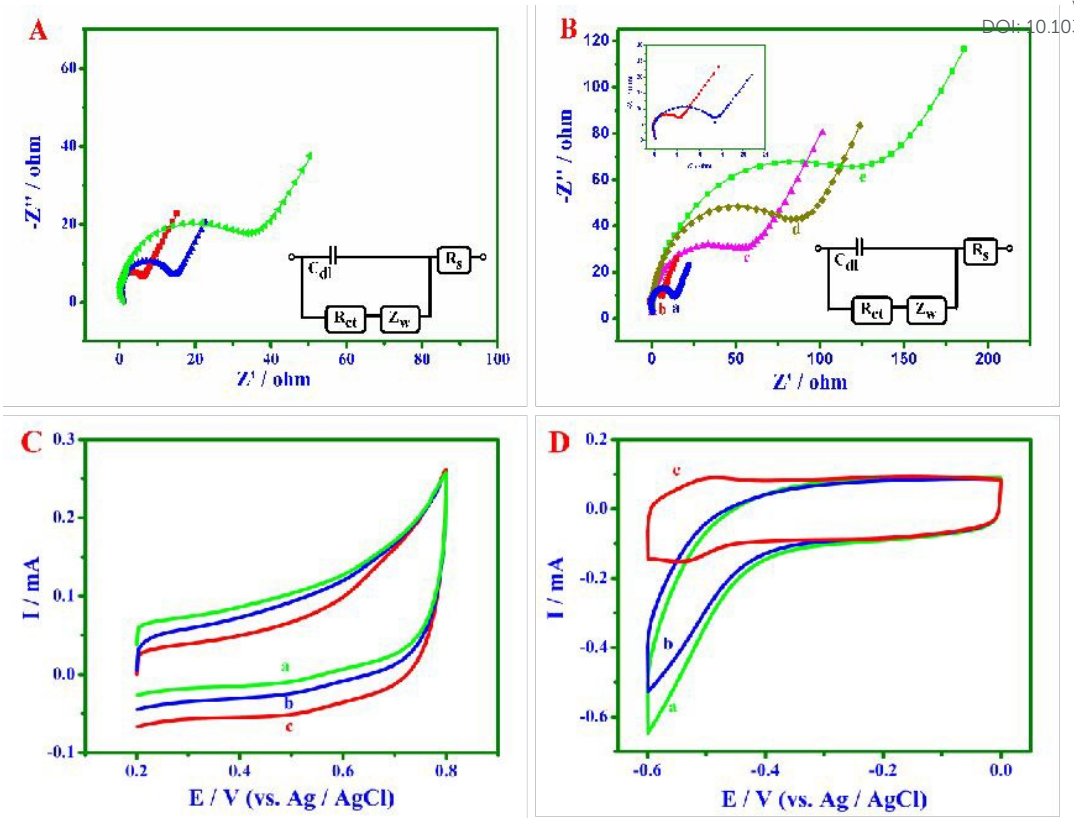

Fig 3. (A) EIS of bare CP (a), N-UHCS/AuNPs/CP (b), BOD/N-UHCS/AuNPs/CP (c); (B) EIS of bare CP (a), N-UHCS/AuNPs/CP (b), DNA1/GOD/N-UHCS/AuNPs/CP (c), SiO_2@AuNPs-csDNA/DNA1/GOD/N-UHCS/AuNPs/CP (d) and DNA bioconjugate SiO_2@AuNPs-csDNA/DNA1/GOD/N-UHCS/AuNPs/CP bioanode after incubation with 100 ng mL^{-1} PDGF-BB (e); (C) CVs of biocathode saturated with N_2 (a), air (b) and O_2 (c) in PBS (pH 7.4); (D) CVs of the bioanode in PBS (pH 7.4) without 5 mM glucose (a) and with glucose (b). CVs of the bioanode in PBS (pH 7.4) with 5 mM glucose and 0.1 μg mL^{-1} PDGF-BB (c).

3.4. Analytical performance of self-powered aptasensor

When there is no PDGF-BB, the E^{OCV} of the self-powered aptasensor is 0.18 V

View Article Online
DOI: 10.1039/C9TB02574J

(curve a, Fig 4A). When various levels of PDGF-BB are added, the E^{OCV} value gradually increases (curve b-j, Fig 4A) due to the improved mass transfer of glucose. The logarithm of E^{OCV} and PDGF-BB concentration are fitted in the linear range from 0.1 to 2000 ng mL^{-1} (the inset of Fig 4B). The linear equation is E^{OCV} = 0.09 log$c$+ 1.22 (R = 0.995). The detection limit is 21.5 pg mL^{-1} (S/N=3). The performance is superior to many similar methods for PDGF-BB (Table 1)[31-37].

Table 1. Analytical performance of various assays for PDGF-BB detection.

Technique	Strategy	Linear range (pM)	LOD (fM)	Ref.
DPV	Hydrothermalroute assisted	1000-10000000	300	31
BLI	Enzyme-linked aptamer sorbent assay	20000-40000000	3200	32
Fluorescence	Nanogel, Thioflavin T and hairpin DNA	25000-300000	23000	33
SWV	DNA hydrogel	0.01-10000000	3.5	34
DPSV	Sandwich-typereaction	17-1660 000000	8300	35
Fluorescence	Hairpin aptamer probes	10-100 000000	3200	36
ECL	Hydrogen peroxide and UV light irradiation	20000-80 000000	0.013	37
EBFC	Nanomaterials and cruciform DNA hybrids	0.0005 -10	0.15	This work

DPV: differential pulse voltammetry; BLI: Biolayer interferometry; DPSV: differential pulse stripping voltammetry; ECL: Electrogenerated chemiluminescence.

3.5. Specificity, stability, reproducibility and real sample analysis

View Article Online
DOI: 10.1039/C9TB02574J

IgG, TB and CEA were used as interferences to explore the selectivity of the aptasensor. As shown in Fig. 4C, in the absence of target PDGF-BB, the signal responses to IgG (20 ng mL^{-1}), TB (2 ng mL^{-1}) and CEA (5ng mL^{-1}) are lower, almost as low as the blank sample. However, the signals of the mixtures (Mix) containing four species are similar to the target PDGF-BB (100 ng mL^{-1}), indicating good selectivity of the method. The stability of the self-powered aptasensor at a continuous reaction time was studied (Fig. 4D). When the concentration of PGDF-BB is 100 ng mL^{-1}, the E^{OCV} kept almost unchanged after 5-days save, and it still remains 98.63% after two weeks, suggesting good stability. Five biosensors were prepared separately and three different concentrations of PGDF-BB (10, 100, 500 ng mL^{-1}) were detected. The relative standard deviation (RSD) was 6.74%, 8.59% and 4.31%, respectively, suggesting a good reproducibility.

The developed assay was used to determine PDGF-BB in the human serum samples (obtained from Affiliated Hospital of Xinyang Normal University) (Table 2). Five serum samples, three from healthy individuals and two from patients with hepatic fibrosis. The serum samples not only were detected by our biosensor, but also an ELISA method for comparison. As displayed in Table 2, the results of this assay are in good agreement with that of the ELISA method, suggesting the aptasensor has great potential to be applied for PGDF-BB bioassay in clinical diagnosis.

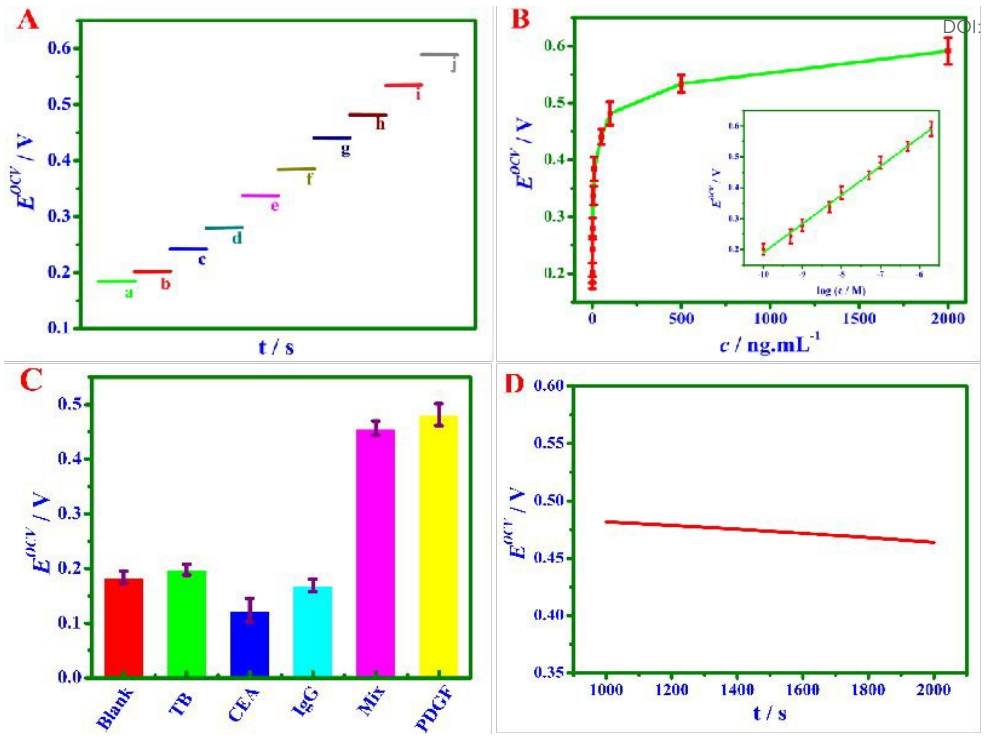

Fig 4. (A) E^{OCV} of the aptasensor in the presence of PDGF-BB with different concentrations (curve a-j :0, 0.1,0.5, 1, 5, 10, 50, 100, 500 and 2000 ng mL^{-1}); (B) The variation of E^{OCV} as a function of PDGF-BB concentrations. Insets is a calibration plot. (C) E^{OCV} of the biosensor in various substances. The "Blank" indicates the condition in the absence of the target and the interfering substances; (D) stability of the aptasensor.

Table 2. Detection of PGDF-BB in human serum samples (n=3).

Serum samples	This biosensor (ng/mL)	ELISA (ng/mL)	Relative errors (%)
1	0.021	0.022	-4.5
2	0.030	0.032	-6.3
3	0.044	0.042	4.8
4	0.298	0.280	6.4
5	0.343	0.369	-7.0

NOTE: Samples from 1 to 3 were from healthy individuals and samples from 4 to 5 were from patients.

View Article Online
DOI: 10.1039/C9TB02574J

4. Conclusion

A sensitive self-powered aptasensor is fabricated for PDGF-BB detection. The aptasensor integrates the large specific surface area and good conductivity of N-UHCS/AuNPs, the high specificity of aptamer and the signal amplification of DNA bioconjugate, and exhibits high sensitivity and excellent specificity towards PDGF-BB detection. In addition, the aptasensor has no need for external power sources and shows the great potential for the clinical applications.

Statement

All experiments in this research work complied with the relevant national laws and regulations, and the ethics committee that approved these experiments was the Institutional Review Board of the affiliated hospital of Xinyang Normal University. Moreover, informed consent was obtained for any experimentation with human subjects.

Acknowledgments

This work was supported by the National Natural Science Foundation of China (21475115), Henan Provincial Science and technology innovation team (C20150026), and Nanhu Scholars Program of XYNU.

References

View Article Online
DOI: 10.1039/C9TB02574J

1 S. Cosnier, A.J. Gross and Goff.A. Le, J. Power Sources, 2016, 325, 252-263.

2 Y.X. Chen , W.H. Ji, K. Yan, J. Gao and J. D. Zhang, Nano Energy, 2019.

3 P.P. Gai, C.C. Gu, T. Hou and F. Li, Anal. Chem., 2017, 89, 2163-2169.

4 C.C. Gu, X.K. Kong, X.J. Liu, P.P. Gai and F. Li, Anal. Chem., 2019, 91, 8697-8704.

5 P.P. Gai, C.C. Gu, T. Hou and F. Li, ACS Appl. Mater. Inter., 2018, 10, 9325-9331.

6 C.C. Gu, P.P. Gai, L. Han, Q.Y. Liu and F. Li, Chem. Commun. 2018, 54, 5438-5441.

7 S. Li, Y. Wang and S. Ge, Biosens. Bioelectron., 2015, 71, 18-24.

8 L.L Wang, H.H. Shao and W.J. Wang, Nano energy, 2018, 44, 95-102.

9 P.P. Gai, Y.S. Ji and W.J. Wang, Nano Energy, 2016, 19., 541-549.

10 X.H. Pang, C. Cui, M.H. Sua, Y.G. Wang, Q. Wei and W.H. Tan, Nano energy, 2018, 46, 101-109.

11 H.M. Meng, H. Liu and H. Kuai, Chem. Soc. Rev., 2016, 45, 2583-2602.

12 C.C. Gu, P.P. Gai, T. Hou, H.Y. Li, C.H. Xue and F. Li, ACS Appl. Mater. Inter., 2017, 9, 35721-35728.

13 L.Y. Fu, J.J. Liu, Z.Q. Hu and M. Zhou, 2018, 30, 2535-2550.

14 Y. Yang, Y. Huang and C. Li, Anal. Chim. Acta, 2019, 1055, 90-97.

15 J. Guo, C. Yuan and Q. Yan, Biosens. Bioelectron., 2018, 105, 103-108.

16 Y.H. Wang, Y.X. Chen, X. Wu and K.J. Huang, Colloid. Surface, 2018, 172, 407-413.

View Article Online
DOI: 10.1039/C9TB02574J

17 Y.X. Chen, K.J. Huang, F. Lin and L.X. Fang, Talanta, 2017, 175, 168-176.

18 Y.H. Wang, K.J. Huang, X. Wu, Y.Y. Ma, D.L. Song, C.Y. Du and S.H. Chang, J. Mater. Chem. B, 2018, 6, 2134-2142.

19 Y.X. Chen, K.J. Huang, L.L. He and Y.H. Wang, Biosens. Bioelectron., 2018, 100, 274-281.

20 H.L. Shuai, X. Wu and K.J. Huang, J. Mater. Chem. B, 2017, 5, 5362-5372.

21 L. Ge, X.M. Sun, Q. Hong and F. Li, ACS Appl. Mater. Inter., 2017, 9, 13102-13110.

22 X.Z. Wang, T. Hou, T.T. Lu and F. Li, Anal. Chem., 2014, 86, 9626-9631

23 Y.X. Chen, K.J. Huang and L.L. He, Biosens. Bioelectron., 2018, 100, 274-281.

24 S.J. Ye, X.M. Zhai and Y.Y. Wu, Biosens. Bioelectron., 2016, 79, 130-135.

25 L. Hong, F. Zhou and D. Shi, Biosens. Bioelectron., 2017, 95, 152-159.

26 W. Yang, W. Yang and F. Ding, Carbon, 2017, 111, 419-427.

27 G. Zhou and Y. A. Zhao, Adv. Energy Mater., 2015, 5, 1402263.

28 S. Azzouzi, W.C. Mak and K. Manthiram, Biosens. Bioelectron., 2017, 92, 154-161.

29 L.L. Xing, G.G. Zhao, K.J. Huang and X. Wu, Dalton Transactions, 2018, 47, 2256-2265.

30 D. Zhang, Y. Guo and Z. Zhao, Appl Catal B: Environ., 2018, 226, 1-9.

31 L.X. Fang, K.J. Huang and Y. Liu, Biosens. Bioelectron., 2015, 71, 171-178.

32 S. Gao, X. Zheng and J. Wu, Biosens. Bioelectron., 2018, 102, 57-62.

33 Z. Zhang, J. Han and Y. Li, Sensor. Actuat. B Chem., 2018, 277, 179-185.

View Article Online
DOI: 10.1039/C9TB02574J

34 Y., Li, M. Chang and Z. Wu, Anal. Chem., 2018, 90, 8241-8247.

35 W. Song, H. Li, H. Liang, W.B. Qiang and D.K. Xu, Anal. Chem., 2014, 86, 2775-2783.

36 M. Zou, D. Li and R. Yuan, J. Mater. Chem. B., 2018, 6, 4146-4150.

37 H.F. Xu, S.J. Liang, X. Zhu, X.Q. Wu, Y.Q. Dong, H.S. Wu, S.J. Ye, X.M. Zhai and Y.W. Chi, Biosens. Bioelectron., 2017, 92, 695-701.